Synthesis and characterisation of Thio-H, a new excitation and emission ratioable fluorescent Ca^{2+}/Mg^{2+} indicator with high brightness

Els Cielen,[a] Agnieszka Stobiecka,[a,b] Abdellah Tahri,[a] Georges J. Hoornaert,[a] Frans C. De Schryver,[a] Jacques Gallay,[c] Michel Vincent[c] and Noël Boens*[a]

[a] *Department of Chemistry, Katholieke Universiteit Leuven, Celestijnenlaan 200F, 3001 Heverlee, Belgium. E-mail: Noel.Boens@chem.kuleuven.ac.be; Fax: + 32-(0)16-327 990*
[b] *Institute of General Food Chemistry, Technical University Lodz, ul Stefanowskiego 4/10, 90-924 Lodz, Poland*
[c] *Laboratoire pour l'Utilisation du Rayonnement Electromagnétique, Centre Universitaire Paris-Sud, 91405 Orsay, France*

Received (in Cambridge, UK) 2nd August 2001, Accepted 5th April 2002
First published as an Advance Article on the web 8th May 2002

A new fluorescent ratiometric indicator for Ca^{2+} and Mg^{2+}, tricaesium salt of {2-[bis(carboxymethyl)amino]-5-(5-phenylthiophen-2-yl)phenoxy}acetic acid, Thio-H, has been synthesised and evaluated for its cation binding properties *via* fluorimetric titrations. Thio-H has the interesting property of being both excitation and emission ratioable, expanding the range of possible applications. The *in vitro* dissociation constant, K_d, measured at 20 °C in 100 mM KCl, pH 7.20 for the Ca^{2+}–Thio-H complex is 45 ± 13 μM; for Mg^{2+}–Thio-H a K_d value of 5.6 ± 0.6 mM is found. The free form of Thio-H has a high fluorescence quantum yield (0.74), which decreases to 0.50 and 0.65 upon binding to Ca^{2+} and Mg^{2+}, respectively. Measurements under physiological conditions show that increasing the temperature from 20 to 37 °C decreases the affinity of Thio-H for Ca^{2+}. Changing the pH from 7.05 to 7.40 does not affect the K_d value of the Mg^{2+} complex but it increases somewhat the affinity of the probe for Ca^{2+}. In the presence of 1 mM Mg^{2+}, the Ca^{2+} affinity of Thio-H decreases (K_d = 126 ± 46 μM at 20 °C, pH 7.05). Time-resolved fluorescence measurements confirm that the inflection point in the fluorimetric titration curve can be correctly assigned to K_d. Since the dissociation constant for the Mg^{2+}–indicator complex falls within the intracellular $[Mg^{2+}]$ domain, while the K_d value for Ca^{2+} is well above the basal Ca^{2+} levels, Thio-H has potential applications as a Mg^{2+} indicator. The low affinity for Ca^{2+} can be exploited for detecting intracellular Ca^{2+} levels in the micromolar range, on condition that $[Mg^{2+}]_i$ remains practically constant during the measurements. Thio-H provides an excellent addition to the commercial ratiometric low-affinity Ca^{2+} indicators Mag-fura-2, Mag-fura-5, Mag-indo-1, Fura-FF, and BTC.

Introduction

The calcium ion is one of the most important and widespread intracellular ions. Cytosolic Ca^{2+} regulates many cellular processes, ranging from muscle contraction, neuronal signalling, secretion, fertilisation, cell division, to metabolism and cell death.[1] Cells at rest have a free intracellular Ca^{2+} concentration of about 100 nM; in active cells, this level can rise to well over 1 μM. The development of fluorescent indicators by Tsien and colleagues entailed a real breakthrough in the elucidation of intracellular calcium dynamics.[2] Although the vast majority of experiments involves the measurement of cytoplasmic Ca^{2+} concentrations, low-affinity Ca^{2+} indicators are very suitable for the determination of Ca^{2+} in intracellular compartments[3] or for monitoring steep increases in intracellular $[Ca^{2+}]$.[4] Since Ca^{2+} concentrations around 1 μM produce almost complete binding saturation of the most frequently used Ca^{2+} indicator Fura-2,[5] but only very low fractional saturation of the low-affinity analog Mag-fura-2,[6] a series of indicators based on the tricarboxylate chelator APTRA (*o*-aminophenol-*N*,*N*,*O*-triacetic acid) with low affinity for Ca^{2+} has been developed.[7] APTRA-based indicators are suitable for detecting elevated Ca^{2+} levels and are sensitive also to Mg^{2+} concentrations from 0.1 to 6 mM, the commonly found range of intracellular free Mg^{2+} levels. Typical physiological Ca^{2+} concentrations (10 nM–1 μM) do not usually interfere with Mg^{2+} measurements because of the relatively low affinity of the APTRA-based indicators for Ca^{2+}. Some of the commercial fluorescent indicators for detecting changes in intracellular $[Ca^{2+}]$ in the range of > 1 μM (BTC, Fura-FF, Mag-fura-2, Mag-fura-5, Mag-indo-1)[7] exhibit spectral shifts upon ion binding, allowing dual-wavelength ratiometric measurements. Such ratiometric indicators allow a more reliable measurement of intracellular $[Ca^{2+}]$ than *via* single wavelength indicators, because the use of a ratio minimises the effect of artefacts (uneven indicator loading, uneven cell thickness, photobleaching, and indicator leakage from the cell) that are unrelated to changes in intracellular $[Ca^{2+}]$. It is obvious that new fluorescent ratiometric Ca^{2+}/Mg^{2+} indicators can provide an interesting addition to the list of existing Ca^{2+}/Mg^{2+} indicators.

Therefore, we have developed Thio-H **1**, tricaesium salt of {2-[bis(carboxymethyl)amino]-5-(5-phenylthiophen-2-yl)phenoxy}acetic acid (Fig. 1), a new ratiometric fluorescent indicator

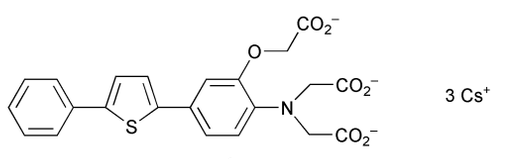

1

Fig. 1 Structure of Thio-H **1**.

DOI: 10.1039/b107042h

for Ca^{2+}/Mg^{2+}, consisting of the tricarboxylate chelator APTRA, linked *via* a Stille reaction to an arylthiophene fluorophore.

In addition to the description of the synthesis of Thio-H, we also report its spectroscopic and Ca^{2+}/Mg^{2+} binding properties. The influence of temperature and pH on the spectral parameters and the complex formation is investigated. Furthermore, a test based on time-resolved fluorescence measurements indicates that the inflection point in the fluorimetric titration curve is correctly assigned to K_d.[8]

Theory

Determination of K_d from direct fluorimetric titration

The expression of the fluorescence signal F as a function of the ion concentration has been derived by Kowalczyk *et al.*[9] for the case of a 1 : 1 complex between a fluorescent indicator and a cation. This expression can be modified by taking into account the formation of an n : 1 ion–indicator complex (n denotes the stoichiometry of the formed complex, Scheme 1). Consider a

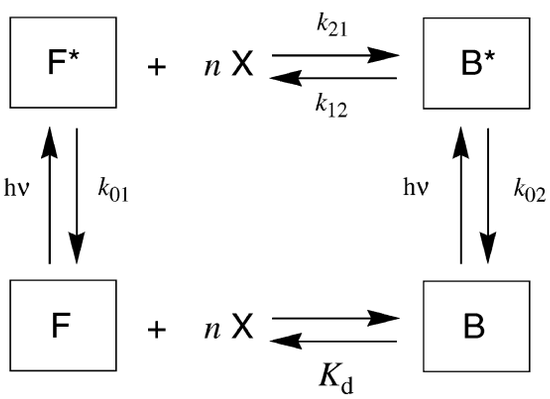

Scheme 1 Kinetic scheme of an intermolecular two-state excited-state system.

photophysical system consisting of the free form of the indicator (F) which in the ground state can undergo a reversible association with cation X to form an n : 1 ion–indicator complex [*i.e.*, the bound form (B) of the indicator]. The association–dissociation is described by the ground-state dissociation constant K_d [eqn. (1)], assuming an n : 1 stoichiometry between X and F,

$$K_d = [F][X]^n/[B] \quad (1)$$

in which [ ] denote molarities. It should be emphasised that Scheme 1 depicts only the overall association–dissociation between an indicator and a cation,[10] so that K_d represents the composite dissociation constant. In Scheme 1, it is further assumed that only species F and B absorb light at the excitation wavelength λ_{ex} to create the corresponding excited-state species F* and B*, which can decay by fluorescence (F) and non-radiative (NR) processes. The composite rate constant for deactivation of species F* is denoted by k_{01} (= $k_{F1} + k_{NR1}$) and by k_{02} for species B*. The overall rate constant describing the association F* + n X ⟶ B* is represented by k_{21}, while the overall rate constant for the dissociation of B* into F* and n X is denoted by k_{12}.

If the system depicted in Scheme 1 is excited with light of constant intensity, and if the absorbance of the sample is less than 0.1, and moreover, if one assumes that the intermediate complexes (between F and one or more cations) are present in concentrations low enough to give only a negligible contribution to the total fluorescence intensity, and that the rate of cation binding in the excited state can be neglected, the total fluorescence signal $F(\lambda_{ex},\lambda_{em},[X])$ at cation concentration [X], due to excitation at λ_{ex} and observed at emission wavelength λ_{em} can be expressed by eqn. (2)[10]

$$F(\lambda_{ex},\lambda_{em},[X]) = \frac{[X]^n F_{max} + K_d F_{min}}{K_d + [X]^n}, \quad (2)$$

where F_{min} represents the fluorescence signal of the free form F* of the indicator, and F_{max} denotes the fluorescence signal of the bound form B*. F_{min} and F_{max} thus correspond to fluorescence signals at minimum and maximum X concentration. Fitting eqn. (2) to the fluorescence data F as a function of [X] yields values for K_d, n, F_{min}, and F_{max}.

Eqn. (2) can be linearised in the form of a Hill plot [eqn. (3)],

$$\log \frac{F - F_{min}}{F_{max} - F} = n\log[X] - \log K_d, \quad (3)$$

from which values for n and K_d can be derived. Since fitting eqn. (2) to the fluorescence data F is a better way for recovering reliable estimates for F_{min}, F_{max}, K_d, and n, we have used this fitting method for obtaining K_d and n values.

Determination of K_d from ratiometric fluorimetric titration

In biological experiments, it is often difficult to keep the analytical indicator concentration constant during the recording of F, F_{min}, and F_{max} because of bleaching and leakage of the fluorescent indicator from cells. In such a case, the ratiometric method, first described by Grynkiewicz *et al.*,[5] is the method of choice. For each concentration of X, one can record the ratio of the fluorescence signals (i) either at two different excitation wavelengths and a common emission wavelength, or (ii) at two different emission wavelengths and a single excitation wavelength.

For the system depicted in Scheme 1, the plot of the ratio $R(\lambda_{ex}^1/\lambda_{ex}^2, \lambda_{em}, [X]) = F(\lambda_{ex}^1, \lambda_{em})/F(\lambda_{ex}^2, \lambda_{em})$ obtained from dual excitation wavelengths at a common observation wavelength as a function of $-\log[X]$ may have multiple inflections, unless the rate of excited-state association can be neglected.[11] (This condition can be verified by the constancy of the fluorescence decay times within the range of used [X];[8] see section on Time-resolved fluorescence). When the excited-state association rate is negligible, we have

$$R(\lambda_{ex}^1/\lambda_{ex}^2,\lambda_{em},[X]) = \frac{[X]^n R_{max} + K_d\xi(\lambda_{ex}^2,\lambda_{em})R_{min}}{K_d\xi(\lambda_{ex}^2,\lambda_{em}) + [X]^n} \quad (4)$$

with

$$\xi(\lambda_{ex}^2,\lambda_{em}) = \frac{F_{min}(\lambda_{ex}^2,\lambda_{em})}{F_{max}(\lambda_{ex}^2,\lambda_{em})} \quad (5)$$

Similarly, the ratio $R(\lambda_{ex}, \lambda_{em}^1/\lambda_{em}^2, [X]) = F(\lambda_{ex}, \lambda_{em}^1)/F(\lambda_{ex}, \lambda_{em}^2)$ at dual emission wavelengths due to a common excitation wavelength is given by eqn. (6) when the excited-state association can be neglected:

$$R(\lambda_{ex}, \lambda_{em}^1/\lambda_{em}^2,[X]) = \frac{[X]^n R_{max} + K_d\xi(\lambda_{ex},\lambda_{em}^2)R_{min}}{K_d\xi(\lambda_{ex},\lambda_{em}^2) + [X]^n} \quad (6)$$

with

$$\xi(\lambda_{ex},\lambda_{em}^2) = \frac{F_{min}(\lambda_{ex},\lambda_{em}^2)}{F_{max}(\lambda_{ex},\lambda_{em}^2)} \quad (7)$$

R_{min} is the ratio of the fluorescence intensities at two distinct excitation wavelengths (respectively emission wavelengths) and one emission wavelength (respectively one excitation wavelength) of the free form of the indicator (minimum X concentration), R_{max} the ratio of the fluorescence intensities of the bound form of the indicator (maximum X concentration), and R denotes the ratio of the fluorescence intensities of solutions with intermediate X concentration. Non-linear fitting eqn. (4) to the excitation ratiometric fluorescence data R as a function of [X] yields values for $K_d\zeta(\lambda_{ex}^2, \lambda_{em})$, n, R_{min}, and R_{max}. Since $\zeta(\lambda_{ex}^2, \lambda_{em})$—the ratio of the fluorescence signal of the free form of the indicator over that of the bound form at the indicated wavelengths—is experimentally accessible, a value for K_d can be recovered from ratiometric excitation fluorescence data. In an analogous way, fitting eqn. (6) to the ratiometric emission fluorescence data R as a function of [X] yields values for $K_d\zeta(\lambda_{ex}, \lambda_{em}^2)$, n, R_{min}, and R_{max}. Since $\zeta(\lambda_{ex}, \lambda_{em}^2)$ can be determined from the fluorescence signals of the free and bound forms of the indicator, a value for K_d can be obtained.

Eqns. (4) and (6) can be linearised in the form of a Hill plot:

$$\log \frac{R - R_{min}}{R_{max} - R} = n\log[X] - \log(K_d\xi) \qquad (8)$$

with ζ given by eqn. (5) for excitation ratiometric fluorescence data and by eqn. (7) for emission ratiometric fluorescence data. Plotting the left-hand side of eqn. (8) as a function of log [X] yields values for n and $K_d\zeta$. Since ζ is experimentally accessible, a value for K_d can be determined. As is the case for direct fluorimetric titrations, non-linear fitting of eqn. (4) or (6) is the recommended approach to recovering reliable estimates for K_d and n. Therefore, we have used this method here.

Time-resolved fluorescence

If the system depicted in Scheme 1 with $n = 1$ is excited by a δ-pulse which does not significantly change the concentrations of the ground-state species (*i.e.*, in the low excitation limit), the fluorescence decays are dual exponential [eqn. (9)],[12]

$$f(\lambda_{ex}, \lambda_{em}, t) = a_1\exp(-\tau/t_1) + a_2\exp(-\tau/t_2),\ t \geq 0 \qquad (9)$$

where the amplitudes a_i ($i = 1, 2$) depend on the rate constants k_{ij}, K_d, [X], λ_{ex}, and λ_{em}. The decay times τ_i ($i = 1, 2$), however, depend exclusively on k_{ij} and [X]. If the excited-state association reaction rate is negligible, the decay times become virtually independent of [X] and are given by

$$\tau_1 = 1/k_{01} \qquad (10)$$

$$\tau_2 = 1/(k_{02} + k_{12}) \qquad (11)$$

A relatively simple experimental test based on time-resolved and steady-state fluorescence measurements can be used to assess the possible misevaluation of K_d from fluorimetric titrations due to the excited-state binding reaction.[8] Collecting fluorescence decay traces in the same [X] range as used in the fluorimetric titration and analysing them simultaneously as biexponentials with linked decay times allows one to check the invariance of the decay times. If an inflection occurs in the [X] range of the fluorimetric titration curve F where the decay times are invariant, this inflection point can be correctly associated with pK_d. This means that in this concentration range, the excited-state binding reaction is negligible and therefore does not interfere with the correct determination of K_d from fluorimetric titration. In contrast, the inflection point(s) in the [X] range where the decay times vary cannot be attributed to K_d.

Results

Design of Thio-H

Based on promising spectroscopic properties of the model compound, methyl 4-(5-phenylthiophen-2-yl)benzoate[13] ($\varepsilon_{346\ nm}$ = 9500 M^{-1} cm^{-1},[13] fluorescence quantum yield ϕ_f = 0.36 in methanol), a thiophene containing unit was chosen as fluorophore. The ionophore consists of a derivative of the chelator APTRA. Although the ion cavity formed by this chelating group is of appropriate size to accommodate Mg^{2+},[14] it has a much higher affinity for Ca^{2+} than for Mg^{2+}. This property has been exploited frequently in the design of low-affinity Ca^{2+} indicators.[6,7] It must be noted that APTRA is a good ligand for many cations, *e.g.* Zn^{2+}.[15]

Synthesis

Synthesis of the ionophore 6. Retrosynthetically, two alternative pathways may be proposed for the synthesis of the ionophore **6** starting from *o*-aminophenol **2**: (i) either the bromination is carried out before the introduction of the *N*,*N*,*O*-triacetic acid branches or (ii) the substitution is carried out in the reverse order. The first method has been described in detail in the literature. 5-Bromo-2-aminophenol can be obtained by nitration of *m*-bromophenol,[16] followed by reduction to an amine according to the method of Bellamy and Ou.[17] Since in the first step, the desired isomer is obtained only in 20% yield, this method is not recommendable. Better yields were reported by Gershon *et al.* for the reaction of acylated 2-aminophenol with *N*-bromosuccinimide in a five step protection–deprotection procedure.[18] After bromination, the triacetic acid branches can be introduced as described for the preparation of the Mg^{2+} selective indicator Mag-fura-2. By introducing the *N*,*N*,*O*-triacetic acid branches prior to bromination (ii), we simplified the sequence to a two-step procedure (Scheme 2).

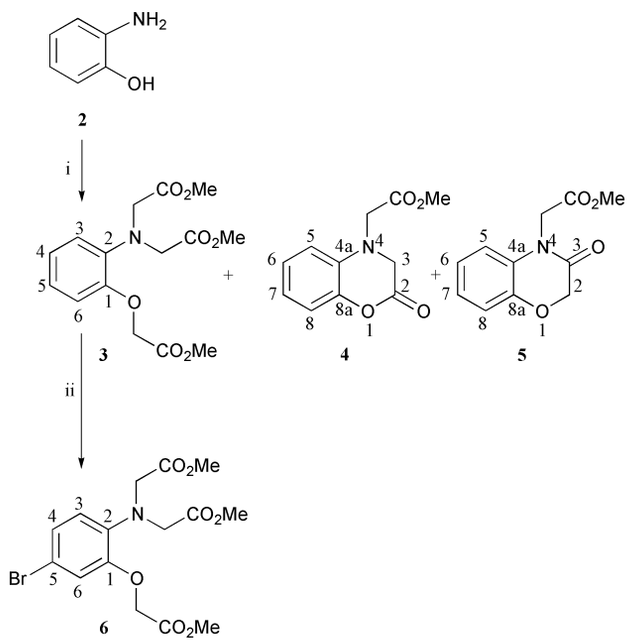

Scheme 2 Synthesis of trimethyl 2-amino-5-bromophenol-*N*,*N*,*O*-triacetate **6**. i: a) 2 equivs. "Proton Sponge", 3 equivs. $BrCH_2CO_2CH_3$, 0.02 equivs. NaI, CH_3CN, 24 h at 70 °C, b) 3 equivs. $BrCH_2CO_2CH_3$, 48 h at 70 °C, ii: 1.1 equiv. NBS, CH_3CO_2H, 30 h at rt.

The *N*,*N*,*O*-triacetic acid branches were introduced onto 2-aminophenol **2** by application of a procedure based on the preparation of the fluorescent magnesium selective chelator Mag-fura-2 (Scheme 2).[6] Compound **2** was heated at 70 °C in acetonitrile in the presence of sodium iodide, 2 equivs. "Proton Sponge" [1,8-bis(dimethylamino)naphthalene] and 3 equivs.

methyl bromoacetate. After 24 hours, another 3 equivs. methyl bromoacetate were added, whereafter the mixture was heated for 48 hours at 70 °C to yield trimethyl 2-aminophenol-*N*,*N*,*O*-triacetate **3**. Significant amounts of a lactone, methyl 2-(2-oxo-2,3-dihydro-4*H*-1,4-benzoxazin-4-yl)acetate **4**, and a lactam, methyl 2-(3-oxo-2,3-dihydro-4*H*-1,4-benzoxazin-4-yl)acetate **5**, were formed by intramolecular cyclisation. Bromination of **3** with *N*-bromosuccinimide gave the desired ionophore **6** in good yields.

Synthesis of the fluorophore 10. The fluorophore was synthesised *via* palladium catalysed cross-coupling reactions (Scheme 3) using the conditions described by Bumagin and

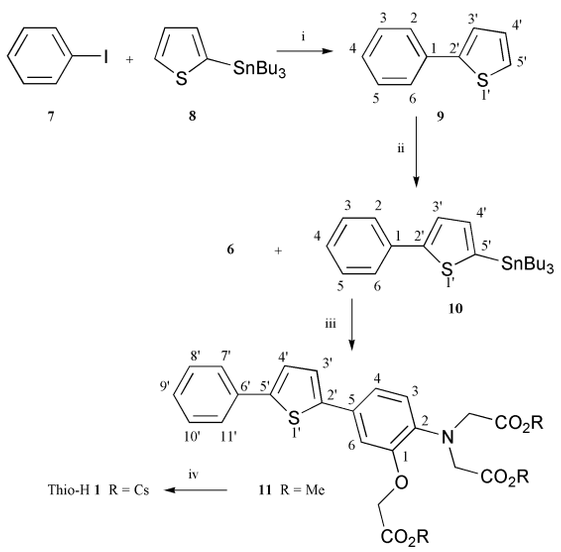

Scheme 3 Synthesis of Thio-H **1**. i: 2 mol% $(MeCN)_2PdCl_2$, DMF, air, rt, ii: a) **9**, BuLi, THF, −78 °C, b) $SnBu_3Cl$, −78 °C, rt, iii: 1 mol% $Pd(PPh_3)_4$, toluene, Ar atmosphere, 15 h reflux, iv: excess CsOH, MeOH, overnight reflux.

Bumagina.[19] The fluorophore skeleton of Thio-H, **9**, was obtained by stirring overnight at room temperature a mixture of 2-(tributylstannyl)thiophene **8** and iodobenzene **7** in DMF under air, catalysed by bis(acetonitrile)dichloropalladium(II). Subsequently, the asymmetrical heterobiaryl compound **9** was converted into the corresponding stannyl derivative **10** by quenching of an *in situ* generated lithium intermediate with tributyltin chloride.[20]

Synthesis of the indicator Thio-H 1. The ionophore **6** was attached to the fluorophore **10** by a palladium-catalysed cross-coupling reaction using the conditions previously described by us for (hetero)aryl–thiophene coupling reactions[10] (Scheme 3). Therefore, the fluorophore **10** was coupled to trimethyl 2-amino-5-bromophenol-*N*,*N*,*O*-triacetate **6** in toluene under argon in the presence of 1 mol% tetrakis(triphenylphosphine)-palladium to yield the ester form of the desired indicator **11**.

Conversion to the water-soluble form. The final reaction step comprised the conversion of the ester **11** into water-soluble form, because the measurements have to be performed in aqueous buffer solutions. The trimethyl ester **11** was converted into the corresponding tricaesium salt **1** by reflux in methanol with a large excess of caesium hydroxide, according to the method of Minta and Tsien[21] and was used as such for the fluorescence measurements. Comparison of the UV spectra of the ester in methanol and the tricaesium salt in water indicates that the fluorophore structure remains unchanged.

Steady-state fluorescence

The spectroscopic measurements were performed on solutions made up to mimic the intracellular milieu of biological cells. The solutions contained 100 mM KCl and 10 mM MOPS (3-[*N*-morpholino]propanesulfonic acid), and were adjusted with potassium hydroxide or hydrochloric acid to the desired pH. The free calcium in the separate solutions was adjusted with Ca^{2+}–nitrilotriacetic acid buffers, as described by Fabiato and Fabiato.[22] Free $[Mg^{2+}]$ was likewise controlled by Mg^{2+}–EGTA [ethylene glycol bis(β-aminoethyl ether)-*N*,*N*,*N*′,*N*′-tetraacetic acid] buffers.[23] The indicator concentration was in the range (3.0–3.3) × 10^{-6} M, yielding an absorbance per cm path length of approximately 0.1 at the absorption maximum.

Excitation and emission spectra. The spectral properties of Thio-H **1** at different pH are summarised in Table 1. As an example, the changes in the excitation spectra that accompany Ca^{2+} and Mg^{2+} binding are illustrated in Figs. 2A and 2B, respectively.

Comparison of these figures shows that the binding of the two divalent metal ions by Thio-H results in a hypsochromic shift of the excitation maximum of about 25 nm relative to the free form. The excitation spectra as a function of Ca^{2+} or Mg^{2+} show a crossover point around 330 nm, which corresponds to a pseudo-isosbestic point. The real isosbestic point (*i.e.* the wavelength where ε for the free and the bound species are equal) was obtained from the absorption spectra and is located around 346 nm.

The emission intensity of the free form is reduced to half when saturated with Ca^{2+} (Fig. 2C), while the position of this maximum remains located around 500 nm. Furthermore, a shoulder shows up around 390–395 nm with increasing $[Ca^{2+}]$, corresponding to the bound form. Increasing magnesium concentrations do not only decrease the fluorescence intensity but also shift the emission maximum to around 489 nm (Fig. 2D). Upon excitation at 363 nm, the emission spectra display a crossover point around 431 nm with Ca^{2+} (Fig. 2C) and one around 451 nm with Mg^{2+} (Fig. 2D). The position of these pseudo-isoemissive points depends on the excitation wavelength. The real isoemissive point can be determined by exciting the indicator at λ_{ex} = isosbestic point[9] and occurs at 446 nm for Ca^{2+} and 472 nm for Mg^{2+}. Thio-H is a very bright fluorescent indicator with a high ϕ_f value for the free as well as the Ca^{2+} or Mg^{2+} bound forms. Because of the large value of the product of the molar extinction coefficient ε and fluorescence quantum yield ϕ_f, Thio-H has a high fluorescence output per indicator, allowing low indicator concentrations to be used,[24] which decreases the cation buffering effects of Thio-H.

Cation binding properties. From the excitation and emission spectra, the dissociation constants K_d and the stoichiometry *n* of the complexes of Thio-H with Ca^{2+} and Mg^{2+} can be determined. The results of the non-linear fitting of the fluorimetric titration data obtained for both cations are shown in Fig. 3. The estimated K_d and *n* values for the Ca^{2+}–Thio-H and Mg^{2+}–Thio-H complexes are summarised in Tables 2 and 3, respectively.

The first method for estimating K_d and *n* is the *direct fluorimetric titration* [see eqn. (2)]. For the Ca^{2+}–Thio-H complex at pH 7.20, K_d and *n* can be determined by monitoring the decrease of the fluorescence excitation intensity at the maximum (Fig. 3A) or by monitoring the decrease of the fluorescence emission intensity at the maximum (figure not shown). K_d values for Ca^{2+}–Thio-H at pH 7.20 are 49 ± 15 μM (excitation) and 56 ± 19 μM (emission) (Table 2), which are in the range of elevated intracellular $[Ca^{2+}]$. The K_d value for Mg^{2+}–Thio-H at pH 7.20, obtained from the fluorescence excitation intensities at 364 nm with the emission wavelength set at 500 nm is 5.7 ± 0.4 mM (Fig. 3C) and 6.3 ± 0.5 mM from fluorescence emission intensities at the same wavelength settings (Table 3). All *n* values indicate a 1 to 1 stoichiometry between indicator and cation (Ca^{2+} and Mg^{2+}). The same non-linear fitting method was used

Table 1 Spectral properties of Thio-H **1** in free and bound (Ca^{2+}/Mg^{2+}) forms, determined at 20 °C in solutions containing 10 mM MOPS and 100 mM KCl. The isosbestic points were determined from the absorption spectra, while the isoemissive points were determined from the emission spectra upon excitation at the isosbestic points

	Absorption [a] λ_{max}/nm			Isosbestic point/nm		Emission [b] λ_{max}/nm			ϕ_f [c]			Isoemissive point/nm	
pH	Free	Ca^{2+}	Mg^{2+}	Ca^{2+}	Mg^{2+}	Free	Ca^{2+}	Mg^{2+}	Free	Ca^{2+}	Mg^{2+}	Ca^{2+}	Mg^{2+}
7.05	351 (31)	332 (31)	335 (30)	345	345	505	505 (390)	488	0.73	0.50	0.57	449	449
7.20	359	335	335	347	347	500	499 (395)	489	0.74	0.50	0.65	446	472
7.40	359	335	335	346	346	500	498 (395)	491	0.75	0.55	0.61	449	472

[a] Numbers in parentheses correspond to the molar extinction coefficients, $\varepsilon_{max} \times 10^{-3}$ (M^{-1} cm^{-1}). [b] Numbers in parentheses correspond to emission wavelength at which a shoulder shows up at increasing [Ca^{2+}]. [c] Estimated error not higher than 10%.

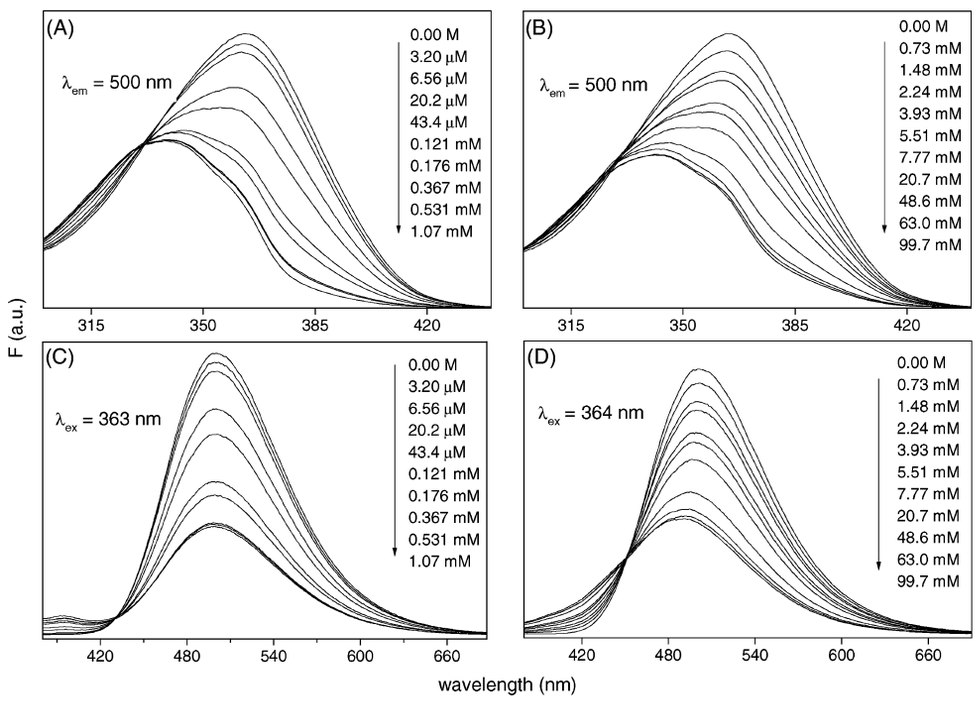

Fig. 2 Fluorescence excitation spectra of Thio-H **1** in solutions containing zero to 1.07 mM Ca^{2+} (A) or zero to 99.7 mM Mg^{2+} (B). Corresponding fluorescence emission spectra of Thio-H **1** as a function of [Ca^{2+}] (C) or [Mg^{2+}] (D). All spectra were recorded at 20 °C in solutions containing 100 mM KCl and 10 mM MOPS pH 7.20.

to estimate K_d and n at other pH values by monitoring changes in fluorescence emission or excitation intensities.

Secondly, for *in vivo* determinations of the intracellular Ca^{2+} and Mg^{2+} concentrations, the *ratiometric method* [see eqns. (4) and (6)] is preferred, because experimental artefacts can be eliminated using this method. For example, for Ca^{2+} binding at pH 7.20 (Table 2), the ratio of the fluorescence excitation intensities at 338 and 363 nm with observation at 500 nm as a function of [Ca^{2+}] was used to estimate K_d and n (Fig. 3B). The estimated K_d value of 67 ± 32 μM agrees well with those obtained *via* the direct method. Again the stoichiometry between probe and Ca^{2+} was 1 to 1. Analogous results were found for Mg^{2+} binding by Thio-H. For example, at pH 7.20, the ratio of the fluorescence intensities at two excitation wavelengths (λ_1 = 341 nm and λ_2 = 364 nm) and at the common observation wavelength (λ_{em} = 500 nm) as a function of [Mg^{2+}] (Fig. 3D) yields K_d = 6.0 ± 0.4 mM and n = 1.05 ± 0.03. When the emission ratiometric mode was used (λ_1 = 482 nm and λ_2 = 500 nm) at the common excitation wavelength (λ_{ex} = 346 nm), the estimated K_d value at pH 7.20 was found to be 5.5 ± 0.5 mM with n = 0.92 ± 0.05 (figure not shown). When n was kept fixed at unity in the fitting, the estimated K_d value was 6.2 ± 0.4 (Table 3). As shown in Tables 2 and 3, the K_d and n values estimated *via* the emission and excitation ratiometric methods are in good agreement with those obtained by the direct titration. The average K_d value for the Ca^{2+} complex at pH 7.20 is 45 ± 13 μM; for the Mg^{2+} complex at the same pH an average K_d value of 5.6 ± 0.6 mM is found.

Influence of pH, temperature and the presence of competitive ions on the binding properties of Thio-H

As the promising *in vitro* properties of Thio-H point towards possible biological applicability, the influence of some physiological conditions on the complexation behaviour with Ca^{2+} was investigated.

According to the results of the fluorimetric titrations, the K_d value estimated for the Ca^{2+}–Thio-H complex (Table 2) is pH dependent: an increase in pH from 7.05 to 7.40 increases somewhat the affinity of the probe for Ca^{2+} (the average K_d drops from 56 ± 5 to 36 ± 3 μM in this pH range). In contrast, in the pH range between 7.05 and 7.40 the average K_d value of Mg^{2+}–Thio-H remains constant around 5.5 mM (Table 3).

The influence of temperature was investigated by carrying out binding measurements for Ca^{2+} at 20 °C and 37 °C. Due to the temperature dependence of the pH of the used buffer, the pH of 7.20 measured at 20 °C decreases to 7.01 at 37 °C. Increasing the temperature causes a decrease of the affinity of Thio-H for Ca^{2+}, in contrast to the observations for the complex formation between Ca^{2+} and the tetracarboxylate chelators EGTA,[25] BAPTA [1,2-bis(*o*-aminophenoxy)ethane-*N*,*N*,*N*′,*N*′-tetraacetic acid],[25] Fura-2,[26,27] and Indo-1.[27]

Table 2 Binding properties of Thio-H **1** with Ca^{2+} determined from fluorimetric titrations. The experimental conditions were the same as in Table 1 except when indicated. All K_d and n values were estimated by non-linear fitting of eqns. (2), (4), or (6)

pH	Experimental excitation and emission wavelengths/nm	K_d/μM	n
7.01 [a]	$\lambda_{ex} = 362$ $\lambda_{em} = 503$	96 ± 18 [b]	1.05 ± 0.05
		90 ± 17 [c]	1.04 ± 0.05
	$\lambda^1_{ex}/\lambda^2_{ex} = 337/362$ $\lambda_{em} = 500$	85 ± 15	1.03 ± 0.04
7.05	$\lambda_{ex} = 360$ $\lambda_{em} = 500$	50 ± 14 [c]	1.02 ± 0.03
	$\lambda^1_{ex}/\lambda^2_{ex} = 350/370$ $\lambda_{em} = 500$	60 ± 4	1.19 ± 0.06
	$\lambda_{ex} = 350$ $\lambda^1_{em}/\lambda^2_{em} = 400/502$	58 ± 6	1.03 ± 0.02
	$\lambda_{ex} = 360$ $\lambda_{em} = 500$	126 ± 46 [c,d]	—
7.20	$\lambda_{ex} = 363$ $\lambda_{em} = 500$	56 ± 19 [b]	1.01 ± 0.09
		49 ± 15 [c]	0.99 ± 0.08
	$\lambda^1_{ex}/\lambda^2_{ex} = 338/363$ $\lambda_{em} = 500$	67 ± 32	1.0 ± 0.1
	$\lambda_{ex} = 335$ $\lambda_{em} = 395$	26 ± 3 [b]	0.87 ± 0.04
		40 ± 3 [b]	1 [e]
	$\lambda_{ex} = 347$ $\lambda_{em} = 500$	43 ± 9 [b]	0.96 ± 0.06
		48 ± 3 [b]	1 [e]
	$\lambda_{ex} = 347$ $\lambda_{em} = 395$	28 ± 3 [b]	0.86 ± 0.03
		45 ± 3 [b]	1 [e]
7.40	$\lambda_{ex} = 364$ $\lambda_{em} = 500$	42 ± 15 [b]	1.1 ± 0.1
		38 ± 14 [c]	1.0 ± 0.1
	$\lambda^1_{ex}/\lambda^2_{ex} = 339/364$ $\lambda_{em} = 500$	34 ± 7	0.87 ± 0.06
	$\lambda_{ex} = 335$ $\lambda_{em} = 395$	31 ± 10 [b]	0.97 ± 0.09
		34 ± 3 [b]	1 [e]
	$\lambda_{ex} = 347$ $\lambda_{em} = 395$	35 ± 10 [b]	1.00 ± 0.07
		36 ± 3 [b]	1 [e]

[a] Measurements performed at 37 °C (pH at 20 °C is 7.20, at 37 °C pH is 7.01). [b] Determined by monitoring the decrease in the fluorescence emission intensity. [c] Determined by monitoring the decrease in the fluorescence excitation intensity. [d] K_d was determined in solutions containing 1 mM Mg^{2+}. [e] n fixed at 1.

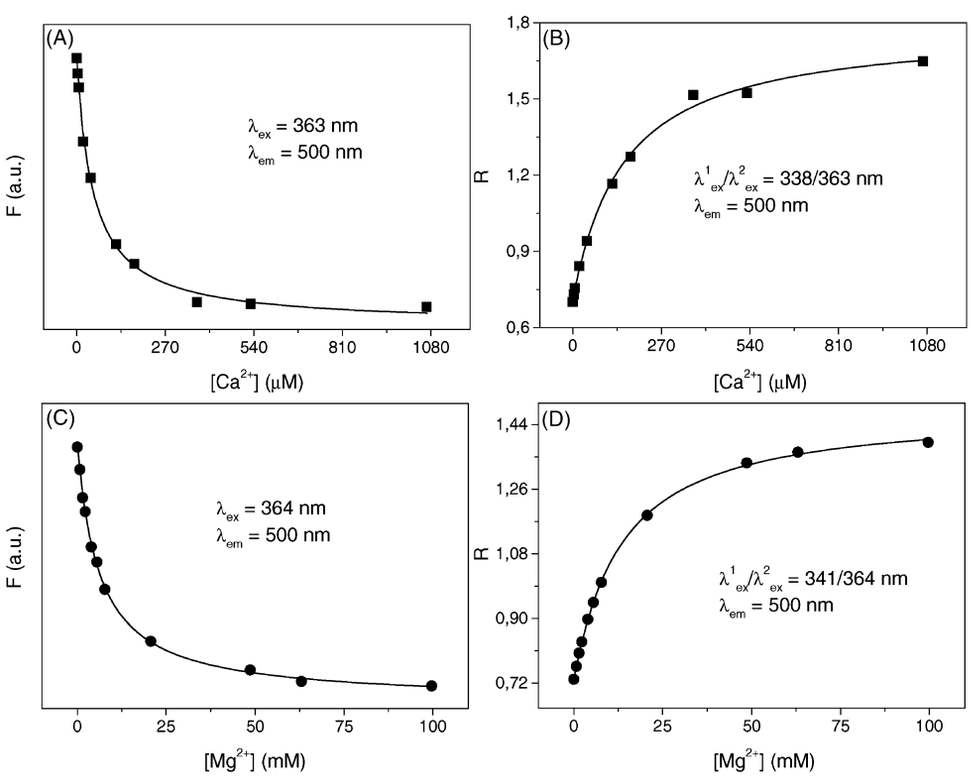

Fig. 3 Estimation of K_d and n for Ca^{2+}–Thio-H **1** and Mg^{2+}–Thio-H **1** complexes using direct fluorimetric titration method [eqn. (2); A and C, respectively] and ratiometric method [eqn. (4); B and D, respectively]. Data were obtained from experiments performed at 20 °C and pH 7.20.

Binding of Thio-H to Ca^{2+} is thus less efficient at higher temperatures (average $K_d = 90 \pm 6$ μM at 37 °C, pH 7.01 *vs.* $K_d = 56 \pm 5$ μM at 20 °C, pH 7.05).

While the presence of physiological Ca^{2+} concentrations does not affect the determination of $[Mg^{2+}]$, on condition that $[Ca^{2+}]_i$ remains relatively constant during the measurements, Ca^{2+} binding is markedly perturbed by physiological levels of Mg^{2+}. From the K_d determination of Ca^{2+}–Thio-H, it was found that the presence of 1 mM Mg^{2+} halves the affinity of Thio-H for Ca^{2+} ($K_d = 126 \pm 46$ μM at 20 °C, pH 7.05). Similar observations were made for the binding of Ca^{2+} by the tetracarboxylate chelator BAPTA [28] and for the affinity of Fura-2 [5] and BTC [29] for Ca^{2+} in the absence and presence of Mg^{2+}.

Because of the importance of pH, temperature and competitive ions in intracellular environments, these parameters should be more extensively investigated if Thio-H turns out to be a useful *in vivo* fluorescent indicator of Ca^{2+}/Mg^{2+}.

Table 3 Binding properties of Thio-H **1** with Mg^{2+} determined from fluorimetric titrations. The experimental conditions were the same as in Table 1. All K_d and n values were estimated by non-linear fitting of eqns. (2), (4), or (6)

pH	Experimental excitation and emission wavelengths/nm	K_d/mM	n
7.05	$\lambda_{ex} = 350$ $\lambda_{em} = 420$	5 ± 2 [c]	1.08 ± 0.03
	$\lambda_{ex}^1/\lambda_{ex}^2 = 350/370$ $\lambda_{em} = 500$	6.1 ± 0.8	1.02 ± 0.07
	$\lambda_{ex} = 350$ $\lambda_{em}^1/\lambda_{em}^1 = 420/500$	5.3 ± 0.9	1.05 ± 0.01
7.20	$\lambda_{ex} = 364$ $\lambda_{em} = 500$	6.3 ± 0.5 [b]	1.00 ± 0.05
		5.7 ± 0.4 [c]	1.00 ± 0.04
	$\lambda_{ex}^1/\lambda_{ex}^1 = 341/364$ $\lambda_{em} = 500$	6.0 ± 0.4	1.05 ± 0.03
	$\lambda_{ex} = 335$ $\lambda_{em} = 400$	4.8 ± 0.4 [b]	0.92 ± 0.06
		5.3 ± 0.3 [b]	1 [a]
	$\lambda_{ex} = 335$ $\lambda_{em}^1/\lambda_{em}^2 = 479/500$	4.7 ± 0.3	0.93 ± 0.05
		5.0 ± 0.3	1 [a]
	$\lambda_{ex} = 346$ $\lambda_{em} = 400$	5.5 ± 0.5 [b]	0.91 ± 0.06
		6.1 ± 0.4 [b]	1 [a]
	$\lambda_{ex} = 346$ $\lambda_{em}^1/\lambda_{em}^2 = 482/500$	5.5 ± 0.5	0.92 ± 0.05
		6.2 ± 0.4	1 [a]
7.40	$\lambda_{ex} = 364$ $\lambda_{em} = 500$	5.2 ± 0.3 [b]	0.91 ± 0.03
		4.6 ± 0.2 [c]	0.89 ± 0.03
	$\lambda_{ex}^1/\lambda_{ex}^2 = 341/364$ $\lambda_{em} = 500$	6.0 ± 0.2	1.05 ± 0.02
	$\lambda_{ex} = 335$ $\lambda_{em} = 500$	6 ± 1 [b]	0.93 ± 0.01
		6 ± 1 [b]	1 [a]
	$\lambda_{ex} = 335$ $\lambda_{em} = 400$	5.2 ± 0.3 [b]	0.94 ± 0.03
		5.6 ± 0.2 [b]	1 [a]
	$\lambda_{ex} = 335$ $\lambda_{em}^1/\lambda_{em}^2 = 479/500$	4.9 ± 0.5	0.94 ± 0.07
		5.2 ± 0.4	1 [a]
	$\lambda_{ex} = 346$ $\lambda_{em} = 500$	5.3 ± 0.5 [b]	0.89 ± 0.07
		5.9 ± 0.5 [b]	1 [a]
	$\lambda_{ex} = 346$ $\lambda_{em} = 400$	5.7 ± 0.2 [b]	0.91 ± 0.02
		6.3 ± 0.3 [b]	1 [a]
	$\lambda_{ex} = 346$ $\lambda_{em}^1/\lambda_{em}^2 = 479/500$	5.8 ± 0.2	0.91 ± 0.02
		6.5 ± 0.3	1 [a]

[a] n fixed at 1. [b] Determined by monitoring the decrease in the fluorescence emission intensity. [c] Determined by monitoring the decrease in the fluorescence excitation intensity.

Time-resolved fluorescence

Before a new fluorescent indicator can be released for *in vivo* measurements, the correct evaluation of K_d has to be checked. In the previous sections, K_d values of the complexes of Thio-H with Ca^{2+} and Mg^{2+} were determined from fluorimetric titration data. However, since fluorescence depends on both ground-state and excited-state parameters, the excited-state association of the cation X with the indicator may influence the value of K_d derived from a fluorimetric titration.[8] A test based on time-resolved measurements has been developed to investigate the possible interference of the excited-state association with the fluorimetric determination of K_d.[8] This test indicates that, if an inflection point occurs in the plot of the fluorescence signal *vs.* −log [X] in the [X] range where both fluorescence decay times are invariant, this inflection point can be associated with the correct K_d. In contrast, inflection points in the [X] range where the decay times vary cannot be attributed to K_d.

To apply this test, time-resolved fluorescence measurements were performed on the system Thio-H–Ca^{2+}. Decay traces of Thio-H at different [Ca^{2+}] ranging from 6.11 μM to 0.73 M were collected at three different sets of excitation/emission wavelengths: (i) λ_{ex} = 330 nm, λ_{em} = 520 nm; (ii) λ_{ex} = 370 nm, λ_{em} = 520 nm; (iii) λ_{ex} = 330 nm, λ_{em} = 480 nm. Each sample was measured twice under the same circumstances. The decay traces of solutions with identical Ca^{2+} concentrations were analysed globally as biexponential functions with the decay times linked over the emission and the excitation wavelengths at each [Ca^{2+}] (Table 4). The short decay time τ_S could not be estimated accurately because its contribution to the total fluorescence is small.[30] The decay traces of all samples within the Ca^{2+} concentration range used for the fluorimetric titration (up to 5.73 × 10^{-4} M) were then analysed globally by linking the fluorescence lifetimes over the different [Ca^{2+}], λ_{ex}, and λ_{em}. Excellent fits were obtained for this extended global biexponential analysis (χ^2 = 1.04, $Z\chi^2$ = 3.12). The recovered lifetimes are τ_L = 3.25 ± 0.01 ns and τ_S = 0.35 ± 0.01 ns. They are represented graphically in Fig. 4. As the decay times remain constant in the range of [Ca^{2+}] used in the fluorimetric titrations, the inflection point in the fluorimetric titrations can be associated with the correct K_d.

Table 4 Global biexponential analysis for each [Ca^{2+}] of the fluorescence decays of Thio-H **1** in the presence of Ca^{2+}. Columns 2 and 3 summarise the globally fitted decay times τ_L (L for long) and τ_S (S for short). # indicates the number of decay traces that were analysed for each concentration. The last two columns describe numerical criteria for the quality of the fits [see eqns. (12) and (13)]

[Ca^{2+}]/M	τ_L/ns	τ_S/ns	#	$Z_{\chi_g^2}$	χ_g^2
1 no added Ca^{2+}	3.25 ± 0.01	0.19	6	0.54	1.01
2 6.11 × 10^{-6}	3.25 ± 0.01	0.16	6	0.42	1.01
3 4.41 × 10^{-5}	3.23 ± 0.01	0.15	6	0.16	1.00
4 5.73 × 10^{-4}	3.24 ± 0.01	0.31 ± 0.05	8 [a]	3.06	1.07
5 4.07 × 10^{-2}	3.32 ± 0.01	0.12 ± 0.04	6	0.19	1.00
6 1.14 × 10^{-1}	3.33 ± 0.01	0.81 ± 0.04	6	2.23	1.06
7 4.86 × 10^{-1}	3.27 ± 0.01	0.66 ± 0.03	6	1.40	1.04
8 7.29 × 10^{-1}	3.30 ± 0.01	0.30 ± 0.01	8 [a]	2.91	1.07

[a] At these concentrations, two extra decay traces were recorded with excitation at 300 nm and emission at 400 nm.

Conclusions

A new ratiometric indicator for Mg^{2+} and Ca^{2+}, Thio-H, has been synthesised *via* a convergent route in which the key steps consisted of Pd catalysed cross-coupling reactions. By modifying the order of reactions, the synthesis of the ionophore synthon could be simplified from an elaborate five-step literature procedure to a more efficient two-step route.

Thio-H provides an excellent addition to the commercially available fluorescent Ca^{2+}/Mg^{2+} indicators, because of its

Table 5 Comparison of spectroscopic properties and K_d (dissociation constant) values of Thio-H **1** and commercial fluorescent low-affinity Ca^{2+} and Mg^{2+} indicators available from Molecular Probes[7]

Indicator (T in °C)	K_d[a]		Ratiometric mode[b]	ϕ_f[c]			ε (at λ_{ex})[d]		
	Ca^{2+}/μM	Mg^{2+}/mM		Free	Ca^{2+}	Mg^{2+}	Free	Ca^{2+}	Mg^{2+}
Mag-fura-2 (22)	25	1.9	Ex 340/380	0.24[6]		0.30[6]	22 (369)[e]	26 (329)[f]	24 (330)[g]
Mag-fura-5 (22)	28	2.3	Ex 340/380				23 (369)[e]	25 (330)[f]	25 (332)[g]
Mag-indo-1 (22)	35	2.7	Em 405/485				38 (349)[e]	35 (328)[f]	33 (330)[g]
BTC (22)	7	—	Ex 400/480		0.12[7]		29 (464)[e]	20 (401)[f]	—
Fura-FF (22)	5.5	—	Ex 340/380				25 (364)[e]	28 (335)[f]	—
Thio-H (20)[h]	45[h]	5.6[h]	[h]	0.74[h]	0.50[h]	0.65[h]	31 (351)[h]	31 (332)[h]	30 (335)[h]

[a] K_d values for the Ca^{2+}–indicator complex have been measured *in vitro* in 100 mM KCl, 10 mM MOPS pH 7.20. K_d values of the Mg^{2+}–indicator complex have been measured *in vitro* in 115 mM KCl, 20 mM NaCl, 10 mM Tris pH 7.05, unless otherwise noted. [b] The indicated wavelengths are given in nm. Ex = excitation ratiometric mode. Em = emission ratiometric mode. [c] Fluorescence quantum yield of the free indicator (zero [Ca^{2+}] and [Mg^{2+}]) and of the Ca^{2+} and Mg^{2+} complexes. [d] Molar extinction coefficient × 10^{-3} M^{-1} cm^{-1} at the indicated excitation wavelength (in nm). [e] Free form measured in aqueous buffer containing 10 mM EGTA. [f] Ca^{2+} bound form measured in aqueous buffer containing a > 10-fold excess of free Ca^{2+} relative to the K_d. [g] Mg^{2+} bound form measured in aqueous buffer containing 35 mM Mg^{2+}. [h] For the experimental conditions of the measurements on Thio-H **1**, see text.

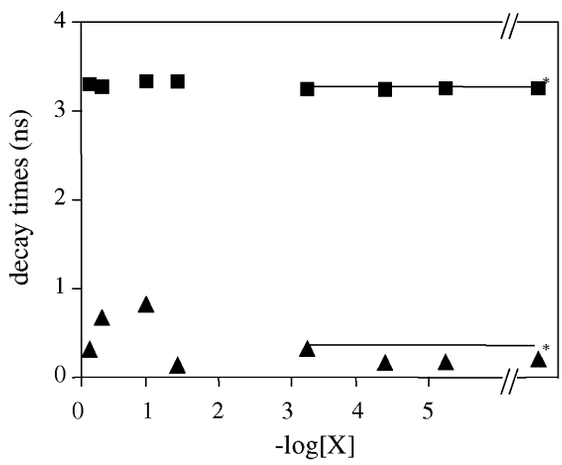

Fig. 4 Decay times of Thio-H **1** as a function of −log [Ca^{2+}]. The symbols ■ and ▲ represent the decay times determined by global biexponential analysis. The symbols marked with * correspond to the samples without added Ca^{2+}. The solid line represents the globally analysed decay times linked over the first four concentrations of Table 4.

interesting property of being both excitation and emission ratioable. An extra advantage is its high fluorescence quantum yield: Thio-H is about three times brighter than the commercial low-affinity Ca^{2+} indicator Mag-fura-2.[6] In Table 5, the spectroscopic properties and K_d values of Thio-H are compared to those of the commercial low-affinity Ca^{2+} indicators.

The dissociation constant for Ca^{2+} is 45 μM at ionic strengths near 0.1 M and pH 7.20; titration with Mg^{2+} yields a dissociation constant of 5.6 mM under the same experimental conditions. Measurements under physiological conditions show that binding of Ca^{2+} to Thio-H is somewhat less efficient at elevated temperatures, while an increase in the pH causes the opposite effect. In the presence of 1 mM Mg^{2+} the Ca^{2+} affinity of Thio-H halves. Time-resolved fluorescence measurements confirm that the inflection point in the fluorimetric titration curve can be correctly assigned to K_d.

Since the dissociation constant for the Mg^{2+}–Thio-H complex falls within the intracellular [Mg^{2+}] range, while the K_d value for Ca^{2+}–Thio-H is well above the basal Ca^{2+} levels, this fluorescent indicator has potential applications as a Mg^{2+} indicator. The low affinity for Ca^{2+} can be exploited for the determination of Ca^{2+} concentrations in the micromolar range, on condition that $[Mg^{2+}]_i$ remains practically constant during the measurements. In the future, it will be investigated whether these promising *in vitro* properties will be confirmed in intracellular environments.

Experimental

Materials and methods

When required, solvents and reagents were dried prior to use. Tetrahydrofuran (THF) and toluene were distilled over sodium. ^{1}H NMR spectra were recorded on a Bruker Avance 300 or a Bruker AMX 400 instrument. The spectra were measured using deuteriochloroform ($CDCl_3$) or deuterated DMSO as solvent; the ^{1}H and ^{13}C chemical shifts are reported in ppm relative to tetramethylsilane or the deuterated solvent as an internal reference; the coupling constants J are given in Hz. Mass spectra were recorded using a Kratos MS50TC instrument and a DS90 data system. IR spectra were taken on a Perkin Elmer 1720 Fourier transform spectrometer. Melting points were determined with a Reichert Thermovar apparatus and are uncorrected.

The absorption measurements were performed on a Perkin Elmer Lambda 6 UV/VIS spectrophotometer. Corrected steady-state excitation and emission spectra were recorded on a SPEX Fluorolog 212. Fluorescence quantum yields of the free and bound forms of the indicators were determined using quinine sulfate in 0.1 N sulfuric acid as reference. The fluorescence quantum yield of this reference was taken to be 0.50 ± 0.02.[31] The samples were measured in Milli-Q water. No correction for the refractive index was necessary. The fluorescence decay traces were collected by the single-photon timing technique[32,33] using the synchrotron radiation facility SUPER-ACO (Anneau de Collision d'Orsay at LURE, France) as described elsewhere.[34] The storage ring provides vertically polarised light pulses with a full width at half maximum of ≈ 500 ps at a frequency of 8.33 MHz in double bunch mode. A Hamamatsu microchannel plate R1564U-06 was utilised to detect the fluorescence photons under magic angle (54° 44′). The instrument response function was determined by measuring the light scattered by glycogen in aqueous solution at the emission wavelength. All decay traces were collected in 1K channels of a multichannel analyser and contained approximately 2 × 10^3 peak counts. The time increment per channel was 30 ps.

Data analysis

The existing general global analysis program[35] based on Marquardt's algorithm[36] was used to obtain estimates of the decay times τ_i (i = 1, 2) [eqn. (9)].

The fitting parameters were determined by minimising the global reduced chi-square χ^2_g:

where the index l sums over q experiments, and the index i

$$\chi^2_g = \sum_l^q \sum_i w_{li}(y^o_{li} - y^c_{li})^2/v \qquad (12)$$

sums over the appropriate channel limits for each individual experiment. y_{li}^{o} and y_{li}^{c} denote respectively the experimentally measured (observed) and fitted (calculated) values corresponding to the i^{th} channel of the l^{th} experiment. w_{li} is the corresponding statistical weight. v represents the number of degrees of freedom for the entire multidimensional fluorescence decay surface. χ_g^2 and its corresponding $Z_{\chi_g^2}$ [eqn. (13)] provide numerical goodness-of-fit criteria for the entire fluorescence decay surface.

$$Z_{\chi_g^2} = (\chi_g^2 - 1)(\tfrac{1}{2}\nu)^{\frac{1}{2}} \quad (13)$$

Using $Z_{\chi_g^2}$ the goodness-of-fit of analyses with different v can be readily compared. The additional criteria that were used to judge the quality of the fits are described elsewhere.[33] Standard error estimates were obtained from the parameter covariance matrix available from the analysis. All quoted errors are one standard deviation.

Synthesis

Trimethyl 2-aminophenol-*N*,*N*,*O*-triacetate 3. To a solution of 2-aminophenol **2** (92 mmol, 10 g) in anhydrous acetonitrile (100 mL) were added sequentially "Proton Sponge" [1,8-bis(dimethylamino)naphthalene] (183 mmol, 2 equivs., 39.7 g), methyl bromoacetate (283 mmol, 3 equivs., 43.3 g) and sodium iodide (0.02 equivs., 0.27 g), after which the mixture was heated under argon to 70 °C. After heating for 24 h, methyl bromoacetate (3 equivs., 43.3 g) was added, whereupon the mixture was heated at 70 °C for another 48 h. The reaction mixture was then filtered on Celite and the obtained organic layer was dried over $MgSO_4$. After evaporation of the solvent, the crude product was chromatographed on silica (CH_2Cl_2–AcOEt, 95 : 5), yielding pale yellow crystals (15%); mp 75 °C; ν_{max}(KBr)/cm^{-1} 3025 (CH_3, CH_2, CH), 1736 (CO), 1609, 1567, 1502 (Ar); δ_H($CDCl_3$) 3.70 (6 H, s, CH_3(N)), 3.78 (3 H, s, CH_3(O)), 4.24 (4 H, s, CH_2(N)), 4.70 (2 H, s, CH_2(O)), 6.85 (4 H, m, Ar); δ_C($CDCl_3$) (Scheme 2) 51.7 (CH_3(N)), 52.1 (CH_3(O)), 53.6 (CH_2(N)), 66.2 (CH_2(O)), 114.9 (6-C), 119.9 (3-C), 122.6 (5-C), 122.7 (4-C), 139.5 (2-C), 149.7 (1-C), 169.4 (CO(O)), 171.8 (CO(N)); *m*/*z* 325 ($M^{+\bullet}$, 24%), 266 ($M^{+\bullet}$ − CO_2Me, 100).

Besides compound **3**, two cyclic side products were formed. A lactone, **methyl 2-(2-oxo-2,3-dihydro-4*H*-1,4-benzoxazin-4-yl)acetate 4**, was isolated in 23% yield; ν_{max}(KBr)/cm^{-1} 3018, 2952 (CH_3, CH_2, CH), 1778, 1739 (CO), 1613, 1591, 1507 (Ar); δ_H($CDCl_3$) (Scheme 2) 3.76 (3 H, s, CH_3), 4.68 and 4.69 (2 H, s, CH_2 and 2 H, s, 3-H), 6.85 (4 H, m, Ar); δ_C($CDCl_3$) 50.2 (CH_3), 50.8 (CH_2), 51.4 (3-C), 115.7 (8-C), 118.9 (5-C), 122.3 (7-C), 122.5 (6-C), 136.4 (4a-C), 145.6 (8a-C), 167.2 (2-C), 170.2 (CO(O)); *m*/*z* 221 ($M^{+\bullet}$, 64%), 162 ($M^{+\bullet}$ − CO_2Me, 60). Furthermore, a lactam, **methyl 2-(3-oxo-2,3-dihydro-4*H*-1,4-benzoxazin-4-yl)acetate 5**, was isolated in 35% yield. ν_{max}(KBr)/cm^{-1} 3013, 2956 (CH_3, CH_2, CH), 1742, (CO), 1687 (amide), 1606, 1597, 1507 (Ar); δ_H($CDCl_3$) (Scheme 2) 3.76 (3 H, s, CH_3), 4.00 (2 H, s, CH_2), 4.09 (2 H, s, 2-H), 6.85 (4 H, m, Ar); δ_C($CDCl_3$) 50.1 (CH_3), 52.3 (CH_2), 66.7 (2-C), 114.3 (8-C), 119.2 (5-C), 123.2 (7-C), 123.4 (6-C), 137.8 (4a-C), 147.7 (8a-C), 165.1 (3-C), 169.6 (CO(O)); *m*/*z* 221 ($M^{+\bullet}$, 64%), 162 ($M^{+\bullet}$ − CO_2Me, 60).

Trimethyl 2-amino-5-bromophenol-*N*,*N*,*O*-triacetate 6. A mixture of trimethyl 2-aminophenol-*N*,*N*,*O*-triacetate **3** (12.4 mmol, 4.02 g) and *N*-bromosuccinimide (13.6 mmol, 2.42 g) (freshly recrystallised from hexane) in acetic acid (25 mL) was stirred at room temperature for 30 h. After evaporation of acetic acid, water (100 mL) and ether (80 mL) were added to the black residue. After separation of the two layers, the aqueous solution was further extracted with ether (80 mL). The ether fractions were combined and dried over $MgSO_4$. After evaporation of the solvent, the yellow oil was chromatographed on silica (CH_2Cl_2–AcOEt, 95 : 5), yielding a crystalline product (3 g, 60 %); mp 58–60 °C; ν_{max}(KBr)/cm^{-1} 2960, 2912 (CH_3, CH_2, CH), 1741 (CO), 1598, 1504 (Ar), 1143, 1060 (C-O-C), 710 (C-Br); δ_H($CDCl_3$) 3.68 (6 H, s, CH_3(N)), 3.76 (3 H, s, CH_3(O)), 4.14 (4 H, s, CH_2(N)), 4.62 (2 H, s, CH_2(O)), 6.7 (1 H, d, *J* 8.5, 3-H), 6.88 (1 H, d, *J* 2.1, 6-H), 7.01 (1 H, dd, *J* 8.5 and *J* 2.1, 4-H); δ_C($CDCl_3$) (Scheme 2) 51.7–52 (CH_3), 53.4 (CH_2(N)), 66 (CH_2(O)), 114.2 (5-C), 117.88 (6-C), 121.08 (3-C), 125.4 (4-C), 138.7 (2-C), 150.19 (C-1), 168.7 (CO(O)), 171.3 (CO(N)); *m*/*z* 404 (MH^+, 88%), 343 ($M^{+\bullet}$ − CO_2Me, − NH, 18), 324 ($M^{+\bullet}$ − Br, 8), 147 ($M^{+\bullet}$ − 3 × CO_2Me, − Br, 16); Found: 403.0285, Calc. for $C_{15}H_{18}BrNO_7$: 403.0267.

2-Phenylthiophene 9. To a mixture of iodobenzene **7** (4.9 mmol, 1 g) and 2-(tributylstannyl)thiophene **8** (4.9 mmol, 1.8 g) in anhydrous DMF (30 mL), $(MeCN)_2PdCl_2$ (2 mol%, 9.8 × 10^{-5} M, 25 mg) was added. After stirring overnight at room temperature, water (100 mL) was added to the reaction mixture, which was then extracted with chloroform (4 × 40 mL). The combined organic layers were washed with water (2 × 20 mL) and then dried over $MgSO_4$. After evaporation, the residue was dissolved in hexane. A black precipitate was formed, which was filtered off. The filtrate was concentrated and the crude product was purified by vacuum distillation (bp 96 °C at 10^{-2} atm). A colourless oil was obtained, which recrystallised upon cooling (0.55 g, 71%); mp 30.8–32.3 °C; ν_{max}(KBr)/cm^{-1} 2921, 2871 (CH), 1602 (Ar); δ_H($CDCl_3$) 7.04 (1 H, dd, *J* 3.9 and *J* 5.1, 4′-H), 7.22 (1 H, dd, *J* 1.2 and *J* 5.1, 5′-H), 7.25 (1 H, m, 4-H), 7.27 (1 H, dd, *J* 1.2 and *J* 3.9, 3′-H), 7.33 (2 H, t, *J* 6.3, 3-, 5-H), 7.58 (2 H, dd, *J* 3.3 and *J* 6.3, 2-, 6-H); δ_C($CDCl_3$) (Scheme 3) 123.0 (3′-C or 4′-C), 124.7 (3′-C or 4′-C), 125.9 (2-C, 6-C), 127.4 (4-C or 5′-C), 127.9 (4-C or 5′-C), 128.8 (3-C, 5-C), 134.4 (1-C), 144.4 (2′-C); *m*/*z* 160 ($M^{+\bullet}$, 100%), 128 ($M^{+\bullet}$ − NS, 19), 115 ($M^{+\bullet}$ − SCH, 49), 102 ($M^{+\bullet}$ − SC_2H_2, 15), 45 (SCH^+, 53); Found: 160.0344, Calc. for $C_{10}H_8S$: 160.0346.

2-Phenyl-5-(tributylstannyl)thiophene 10. In a three-necked flask equipped with a septum and a stopcock, 2-phenylthiophene **9** (8.4 mmol, 1.3 g) was dissolved in anhydrous THF (50 mL). After cooling to −78 °C, a solution of butyllithium (1.2 equivs., 10 mmol) in hexane was added *via* a syringe. The mixture was stirred at −78 °C under argon for 30 min, after which tributyltin chloride (1.2 equivs., 10 mmol, 3.25 g) was added dropwise *via* a syringe. The reaction mixture was stirred at room temperature and then poured into glacial brine (75 mL), which was washed with ether (3 × 75 mL). After evaporation, the unreacted starting material was removed by vacuum distillation, after which the residue was purified by column chromatography (Al_2O_3; hexane). A yellow oil was obtained (80%); ν_{max} (KBr)/cm^{-1} 2958–2853 (CH_3, CH_2, CH), 1599 (Ar), 1572 (Ar); δ_H($CDCl_3$) 0.91 (9 H, m, CH_3), 1.12 (6 H, m, CH_2), 1.35 (6 H, m, CH_2), 1.58 (6 H, m, CH_2), 7.19 (1 H, d, *J* 3.37, 3′-H or 4′-H), 7.30 (1 H, m, 4-H), 7.42 (2 H, t, *J* 8.63, 3-, 5-H), 7.47 (1 H, d, *J* 3.37, 3′-H or 4′-H), 7.67 (2 H, dd, *J* 3.21 and *J* 8.63, 2-, 6-H); δ_C($CDCl_3$) (Scheme 3) 8.7 (CH_2Sn), 13.58 (CH_3), 28.95 (CH_2), 30.11 (CH_2), 125.04 (3′-C), 126.45 (2-C, 6-C), 127.4 (4-C), 129.02 (3-, 5-C), 134.8 (1-C), 142.9 (2′-C), 146.0 (5′-C), 150.7 (4′-C); *m*/*z*: 450 ($M^{+\bullet}$, 5%), 393 ($M^{+\bullet}$ − Butyl, 100), 336 ($M^{+\bullet}$ − 2 × Butyl, 54), 279 ($M^{+\bullet}$ − 3 × Butyl, 52), 235 $(Sn(Bu)_2^+$, 15), 177 ($SnBu^+$, 14); Found: 450.1398, Calc. for $C_{22}H_{34}SSn$: 450.1403.

Trimethyl ester of {2-[bis(carboxymethyl)amino]-5-(5-phenylthiophen-2-yl)phenoxy}acetic acid 11. To a solution of 2-phenyl-5-(tributylstannyl)thiophene **10** (1.2 equivs., 1.2 mmol, 0.54 g) in anhydrous toluene (20 mL), trimethyl 2-amino-5-bromophenol-*N*,*N*,*O*-triacetate **6** (1 mmol, 0.34 g) and tetrakis(triphenylphosphine)palladium(0) (1 mol%, 11 mg) were added. The reaction mixture was refluxed for 15 h under argon

atmosphere. After evaporation of toluene, the product was purified on alumina (EtOAc–hexane 30 : 70 with a gradient to pure EtOAc) and recrystallised from chloroform by addition of cold hexane. A yellow powder was obtained (66%); mp 81–83 °C; ν_{max}(KBr)/cm^{-1} 2955, 2924 (CH_3, CH_2), 2855 (CH), 1728 (CO), 1596, 1569, 1492 (Ar); δ_H($CDCl_3$) (Scheme 3) 3.73 (6 H, s, CH_3(N)), 3.80 (3 H, s, CH_3(O)), 4.24 (4 H, s, CH_2(N)), 4.72 (2 H, s, CH_2(O)), 6.89 (1 H, d, *J* 8.32, 3-H), 7.06 (1 H, d, *J* 1.88, 6-H), 7.14 (1 H, d, *J* 3.7, 3′-H or 4′-H), 7.20 (1 H, dd, *J* 1.88 and *J* 8.3, 4-H), 7.24 (1 H, d, *J* 3.7, 3′-H or 4′-H), 7.23–7.27 (1 H, m, 9′-H), 7.37 (2 H, t, *J* 7.46, 8′-, 10′-H), 7.60 (2 H, d, *J* 7.46, 7′-, 11′-H); δ_C($CDCl_3$) 51.8 (CH_3(N)), 52.1 (CH_3(O)), 53.5 (CH_2(N)), 66.2 (CH_2(O)), 112.4 (6-C), 119.8 (3-C), 120.1 (4-C), 123.8 and 123.9 (3′-, 4′-C), 125.4 (7′-, 11′-C), 127.3 (9′-C), 128.8 (8′-, 10′-, 5-C), 134.2 (2-C), 139.0 (6′-C), 142.8 and 143.1 (2′-, 5′-C), 149.5 (1-C), 169.1 (CO(O)), 171.5 (CO(N)); *m*/*z* 483 ($M^{+\bullet}$, 94%), 424 ($M^{+\bullet} - CO_2Me$, 100), 351 ($M^{+\bullet} - 2 \times CO_2Me$, $- CH_2$, 24), 278 ($M^{+\bullet} - 3 \times CO_2Me$, $- 2 \times CH_2$, 18), 235 ($M^{+\bullet}$ $- N(CH_2CO_2CH_3)_2$, $- OCH_2CO_2CH_3$, 11); Found: 483.1361, Calc. for $C_{25}H_{25}NO_7S$: 483.1352.

Tricaesium salt Thio-H 1. This was prepared from compound **11** according to the procedure described by Minta and Tsien.[21] A solution of the ester (1.03×10^{-5} mol) and anhydrous caesium hydroxide (1.03×10^{-4} mol, 10 equivs.) in methanol (3 cm^3) was refluxed overnight. After evaporation of the methanol, the product was dissolved in water (100 cm^3) and used as such for the fluorescence measurements.

Acknowledgements

The authors are indebted to Professor Dr S. Toppet and R. De Boer for the NMR and mass spectra, respectively. K. Van Werde is thanked for assistance with the time-resolved fluorescence measurements. E.C. is an *Aspirant* and N.B. is an *Onderzoeksdirecteur* of the *Fonds voor Wetenschappelijk Onderzoek (FWO)*. A.T. is a postdoctoral fellow at the K. U. Leuven. A.S. thanks the Flemish Ministry of Science and Technology for a postdoctoral fellowship through the Bilateral Scientific and Technological Cooperation Programme (BIL 97/09). The continuing financial support of DWTC through IUAP-4-11 is gratefully acknowledged.

References

1 M. J. Berridge, P. Lipp and M. D. Bootman, *Nature Rev. Mol. Cell Biol.*, 2000, **1**, 11.
2 R. Y. Tsien, *Annu. Rev. Neurosci.*, 1989, **12**, 227; W. J. J. M. Scheenen, A. M. Hofer and T. Pozzan, in *Cell Biology: A Laboratory Handbook, 2*nd Edn., J. E. Celis, Ed., Vol. 3, Academic Press, 1998, p. 363; A. Takahashi, P. Camacho, J. D. Lechleiter and B. Herman, *Physiol. Rev.*, 1999, **79**, 1089.
3 A. M. Hofer and T. E. Machen, *Proc. Natl. Acad. Sci. USA*, 1993, **90**, 2598; V. A. Golovina and M. P. Blaustein, *Science*, 1997, **275**, 1643; G. Csordás, A. P. Thomas and G. Hajnóczky, *EMBO J.*, 1999, **18**, 96; J. Meldolesi and T. Pozzan, *Trends Biochem. Sci.*, 1998, **23**, 10.
4 A. L. Escobar, J. R. Monck, J. M. Fernandez and J. L. Vergara, *Nature*, 1994, **367**, 739; A. M. Hofer, B. Landolfi, L. Debellis, T. Pozzan and S. Curci, *EMBO J.*, 1998, **17**, 1986; A. K. Stout and I. J. Reynolds, *Neuroscience*, 1999, **89**, 91.
5 G. Grynkiewicz, M. Poenie and R. Y. Tsien, *J. Biol. Chem.*, 1985, **260**, 3440.
6 B. Raju, E. Murphy, L. A. Levy, R. D. Hall and R. E. London, *Am. J. Physiol.*, 1989, **256**, C540.
7 R. P. Haugland, *Handbook of Fluorescent Probes and Research Products*, Molecular Probes, Eugene, OR, USA, 8th edn. (CD-version), 2001.
8 A. Kowalczyk, N. Boens, K. Meuwis and M. Ameloot, *Anal. Biochem.*, 1997, **245**, 28.
9 A. Kowalczyk, N. Boens, V. Van den Bergh and F. C. De Schryver, *J. Phys. Chem.*, 1994, **98**, 8585.
10 E. Cielen, A. Tahri, K. Ver Heyen, G. J. Hoornaert, F. C. De Schryver and N. Boens, *J. Chem. Soc., Perkin Trans. 2*, 1998, 1573.
11 V. Van den Bergh, N. Boens, F. C. De Schryver, M. Ameloot, P. Steels, J. Gallay, M. Vincent and A. Kowalczyk, *Biophys. J.*, 1995, **68**, 1110.
12 J. B. Birks, *Photophysics of Aromatic Molecules*, Wiley, New York, 1970.
13 G. Kirsch, D. Prim, F. Leising and G. Mignani, *J. Heterocycl. Chem.*, 1994, **31**, 1005.
14 L. A. Levy, E. Murphy, B. Raju and R. E. London, *Biochemistry*, 1988, **27**, 4041.
15 O. Reany, T. Gunnlaugsson and D. Parker, *J. Chem. Soc., Perkin Trans. 2*, 2000, 1819; O. Reany, T. Gunnlaugsson and D. Parker, *Chem. Commun.*, 2000, 473.
16 H. H. Hodgson and F. H. Moore, *J. Chem. Soc.*, 1926, 155; C. Wright, M. Shulkind, K. Jones and M. Thompson, *Tetrahedron Lett.*, 1987, **28**, 6389; R. P. Hanzlik, P. E. Weller, J. Desai, J. Zheng, L. R. Hall and D. E. Slaughter, *J. Org. Chem.*, 1990, **55**, 2736.
17 F. D. Bellamy and K. Ou, *Tetrahedron Lett.*, 1984, **25**, 839.
18 H. Gershon, D. D. Clarke and M. Gershon, *Monatsh. Chem.*, 1993, **124**, 367.
19 N. A. Bumagin and I. G. Bumagina, *Dokl. Akad. Nauk SSSR*, 1983, **274**(4), 2547.
20 S. Gronowitz, A.-B. Hörnfeldt and Y. Yang, *Chem. Scr.*, 1988, **28**, 281.
21 A. Minta and R. Y. Tsien, *J. Biol. Chem.*, 1989, **264**, 8171.
22 A. Fabiato and F. Fabiato, *J. Physiol. (Paris)*, 1979, **75**, 219.
23 R. Y. Tsien, *Biochemistry*, 1980, **19**, 2396.
24 R. Y. Tsien, in *Fluorescent Chemosensors for Ion and Molecule Recognition*, A. W. Czarnik, Ed., ACS Symposium Series, Washington, 1993, p. 538.
25 S. M. Harrison and D. M. Bers, *Biochim. Biophys. Acta*, 1987, **925**, 133.
26 P. W. Marks and F. R. Maxfield, *Anal. Biochem.*, 1991, **193**, 61.
27 T. J. Shuttleworth and J. L. Thompson, *J. Biol. Chem.*, 1991, **266**, 1411.
28 R. Pethig, M. Kuhn, R. Payne, E. Adler, T. H. Chen and L. F. Jaffe, *Cell Calcium*, 1989, **10**, 491.
29 H. Iatridou, E. Foukaraki, M. A. Kuhn, E. M. Marcus, R. P. Haugland and H. E. Katerinopoulos, *Cell Calcium*, 1994, **15**, 190.
30 L. D. Janssens, N. Boens, M. Ameloot and F. C. De Schryver, *J. Phys. Chem.*, 1990, **94**, 3564.
31 W. R. Dawson and M. W. Windsor, *J. Phys. Chem.*, 1968, **72**, 3251.
32 D. V. O'Connor and D. Phillips, *Time-Correlated Single Photon Counting*, Academic Press, New York, 1984.
33 N. Boens, *Luminescence Techniques in Chemical and Biochemical Analysis*, Eds. W. R. G. Baeyens, D. De Keukeleire and K. Korkidis, Marcel Dekker, New York, 1991, p. 21.
34 O. P. Kuipers, M. Vincent, J. C. Brochon, H. M. Verheij, G. H. De Haas and J. Gallay, *Biochemistry*, 1991, **30**, 8771.
35 N. Boens, L. D. Janssens and F. C. De Schryver, *Biophys. Chem.*, 1989, **33**, 77.
36 D. W. Marquardt, *J. Soc. Ind. Appl. Math.*, 1963, **11**, 431.